

# PREDICTING THE EFFECT OF SHOT PEENING ON WELD FATIGUE LIFE

Se-Tak Chang and F. V. Lawrence, Jr.

*Department of Metallurgy and Mining Engineering, University of Illinois at Urbana-Champaign, Urbana, IL 61801, USA*

## ABSTRACT

An analytical model was developed to predict the effect of shot peening on the fatigue life of a weld. The total fatigue life of a weld was considered to be composed of a crack initiation and crack propagation period. Residual stresses and the material properties of the peened surface were considered in the estimation of the crack initiation life but not in the crack propagation life. The shot-peened weld toe was considered to be a strain hardened and heavily plastic-deformed surface layer with altered material properties and high compressive residual stresses. Fatigue notch factors ( $K_f$ ) were estimated using Peterson's equation and the  $K_f$  maximum concept. The maximum compressive residual stresses at weld toe introduced by shot peening were estimated from experimental data. Neuber's rule was used to determine the local stress-strain behavior and the mean stress established during the set-up cycle at weld toe. Fatigue tests of A514 grade F/E110 steel butt welds in the shot peened and as-welded conditions were conducted to verify the analytically predicted total fatigue lives.

## KEYWORDS

Fatigue of weldments; shot peening; fatigue life predictions; fatigue.

## IMPROVING THE FATIGUE RESISTANCE OF WELDS

The fatigue resistance of welds is generally less than that of the plain plate members which they join. Figure 1 shows the output of a fatigue data bank compiled by Munse (1) for mild steel butt welds. As shown in Fig. 1 for mild steel, the average fatigue strength of plain plate is significantly greater than that of welds. This loss in fatigue life can be reduced by one of several methods: altering the weld geometry, controlling weld residual stresses or by improving the material properties which promote greater fatigue resistance. As will be discussed in this study, shot peening is a very effective post-weld treatment which lengthens the fatigue life by the latter two means. The fatigue resistance of a weldment can never exceed the fatigue life of the plain plate which it joins; therefore, no weld fatigue life improvement scheme can lead to lives in excess of the plain plate fatigue resistance. This fact leads to the concept of maximum recoverable life, the difference between plain plate and weldment fatigue life at a given stress (see Fig. 2).

PREDICTING THE FATIGUE RESISTANCE OF WELDS

To permit the accurate prediction of weldment fatigue resistance and to provide a means of interrelating the parameters which improve the fatigue life of welds, an analytical model for estimating the total fatigue life of welds has been developed (2) which assumes that the total fatigue life of a weldment ( $N_T$ ) is composed of a fatigue crack initiation period ( $N_I$ ) and a fatigue crack propagation period ( $N_p$ ) such that:

$$N_T = N_I + N_p$$

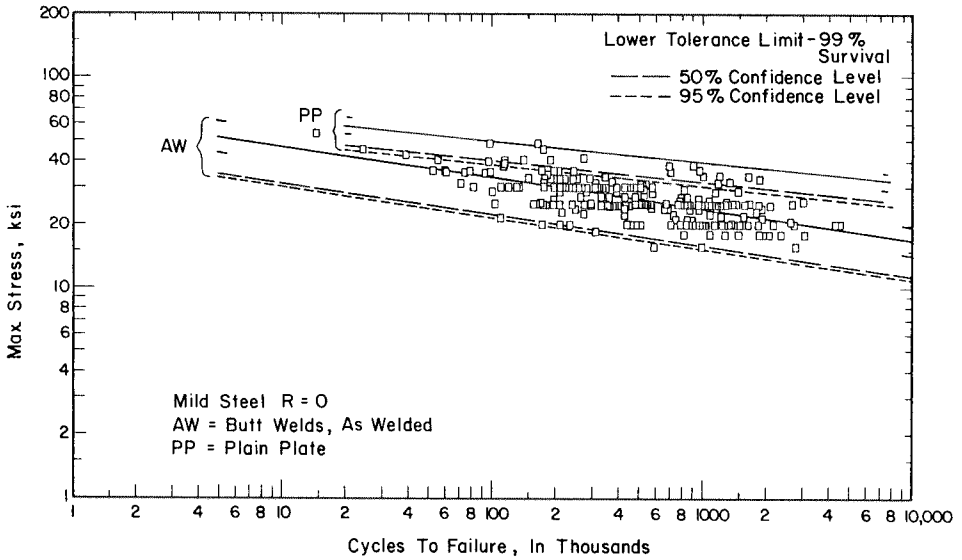


Fig. 1. Stress range versus cycles to failure for mild steel butt welds subjected to zero-to-tension loading. The fatigue resistance of as-welded butt welds is generally less than the fatigue resistance of plain plate.

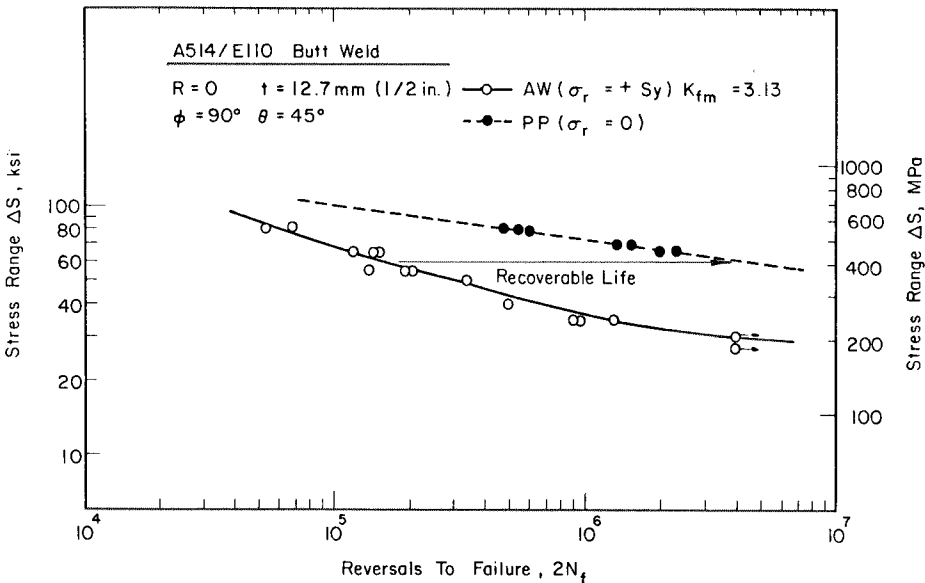


Fig. 2. The maximum recoverable life of ASTM A514/E110 butt welds.

The initiation portion of life ( $N_I$ ) is estimated using strain-control fatigue data and is considered to consist of the number of cycles for the initiation of a fatigue crack(s) and its (their) early growth and coalescence into a dominant fatigue crack. The fatigue crack propagation portion of life ( $N_D$ ) is estimated using (long-crack) fatigue-crack propagation data assuming the "appropriate" value of the initiated crack length ( $a_I$ ).

The base metal of a weld is seldom involved in the fatigue crack initiation process (Fig. 3); most fatigue cracks initiating at internal defects do so in tempered weld metal; toe cracks will initiate in the grain-coarsened heat affected-zone (high wetting angles) or in untempered, highly diluted weld metal (low wetting angles). Test data on weld metal and heat affected zone materials are generally unavailable and difficult to obtain experimentally, but it is possible to estimate roughly the fatigue strength coefficient ( $\sigma_f'$ ), the transition fatigue life ( $2N_{tr}$ ), the fatigue strength exponent ( $b$ ) and the mean stress relaxation exponent ( $k$ ) from hardness (Fig. 4) determined by measurements performed in the region which the fatigue crack is expected to initiate (3).

For long-life fatigue ( $N_I > 10^5$  cycles), cyclic hardening and softening effects can usually be ignored, and generally elastic conditions may be assumed. For such cases,  $N_I$  can account for the major portion of the total fatigue life and can be estimated using the Basquin relationship (4):

$$\sigma_a = (\sigma_f' - \sigma_0) [2N_I]^b \quad (2)$$

where:

$\sigma_a$  is the stress amplitude,

$\sigma_f'$  is the fatigue strength coefficient,

$\sigma_0$  is the mean stress including weld residual as well as remote mean stress,

$2N_I$  is the reversals to fatigue crack initiation, and

$b$  is the fatigue strength exponent.

The notch-root stress amplitude, the stress at the critical region in the weld (weld toe or internal defect), can be taken as  $\Delta S/2 K_f$  so that Eq. 2 becomes:

$$\frac{\Delta S}{2} K_f = (\sigma_f' - \sigma_0) [2N_I]^b \quad (3)$$

where:

$\Delta S$  is the remote stress range, and

$K_f$  is the fatigue notch factor (also  $K_{fmax}$ ).

A difficulty in proceeding with the life estimation calculation suggested by Eq. 3 is determining the appropriate value of  $K_f$  for the weld toe. This difficulty arises from the fact that the notch-root radius of a discontinuity such as the weld toe is unknown and variable. Microscopic examination of weld toes reveals

\*The transition fatigue life,  $N_{tr}$ , is defined as the fatigue life at which the elastic and plastic strains are equal.

that practically any value of radius can be observed (see Fig. 7); thus, notches such as weld toes must be considered to have all possible values of notch-root radius which conclusion has led to the idea of a maximum value of  $K_f$  for a given weld shape,  $K_{fmax}$  (2).  $K_f$  can be estimated using Peterson's equation:

$$K_f = 1 + \frac{K_t - 1}{1 + \frac{a}{r}} \quad (4)$$

where:

$K_t$  is the elastic stress concentration factor,

$a$  is a material parameter ( $\approx 1.08 \times 10^5 S_u^{-2}$ ), for steels (mm),

$r$  is the notch-root radius (mm), and

$S_u$  is the ultimate strength (MPa).

The elastic stress concentration factor ( $K_t$ ) can be estimated using finite element methods as a function of assumed notch root radii ( $r$ ) for a given weld geometry (Fig. 5). Assuming the general form of  $K_t$  for welds (5):

$$K_t = 1 + \alpha (t/r)^{1/2} \quad (5)$$

where:

$\alpha$  is a constant determined by the weld geometry and type of loading and

$t$  is the plate thickness.

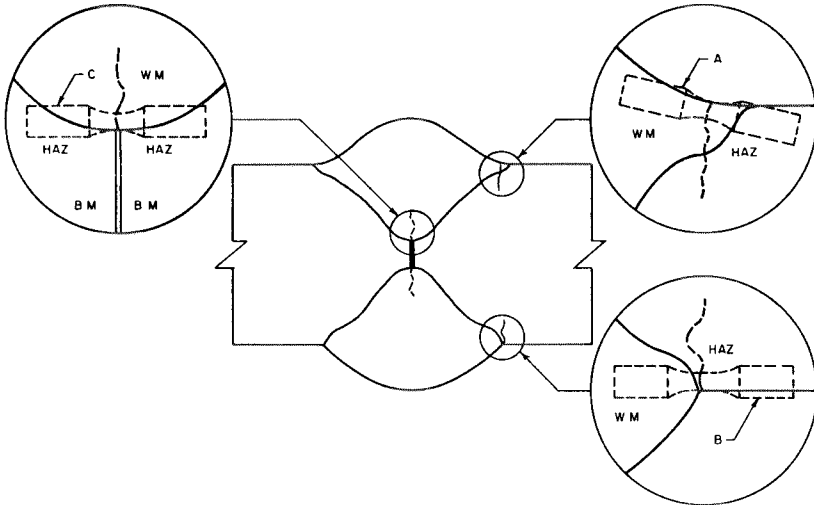


Fig. 3. Typical locations of fatigue crack initiation in a butt weld. Fatigue cracks can initiate: in diluted, untempered weld metal (A); in the heat affected zone close to the line of fusion (B); and in tempered weld metal (C).

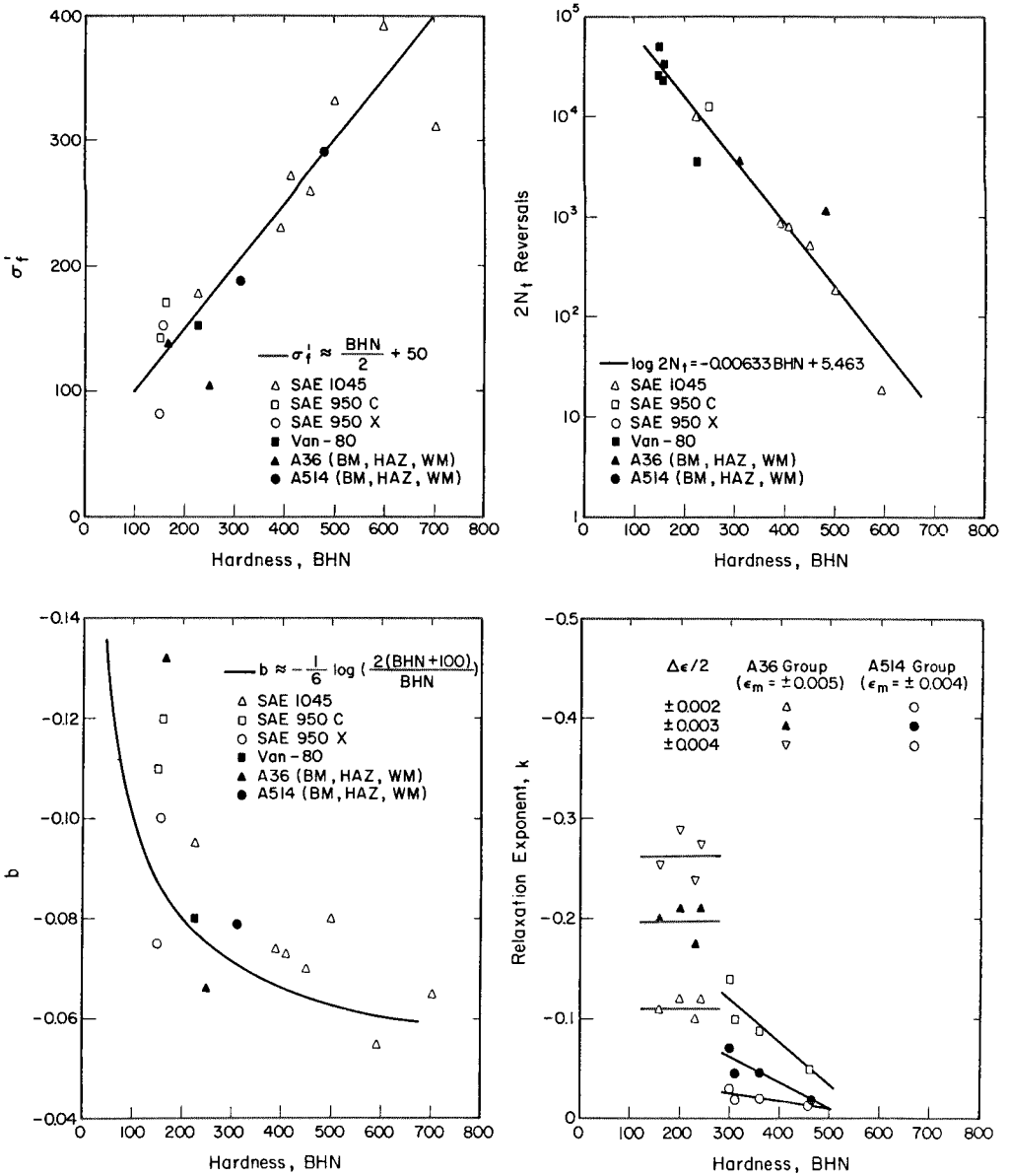


Fig. 4. Variation of  $\sigma_f$ ,  $b$ ,  $2N_{tr}$ , and  $k$  with Brinell Hardness (BHN).

Substituting this into Eq. 4 and differentiating with respect to  $(r)$  to obtain the maximum value of  $K_f$ ,  $K_{fmax}$ :

$$K_{fmax} = 1 + (\alpha/2)(t/a)^{1/2} \approx 1 + .0015\alpha S_u t^{1/2} \quad (\text{for steel}) \quad (6)$$

As seen in Fig. 5,  $K_t$  always increases with decreasing ( $r$ ), but  $K_f$  passes through a maximum ( $K_{fmax}$ ) at  $r_{crit}$  equal to "a" in Peterson's equation (Eq. 4).  $K_{fmax}$  should be the largest possible value of  $K_f$  for the weld shape and material in question. Because "a" is dependent upon the ultimate strength ( $S_u$ ), higher strength steels will have higher values of  $K_{fmax}$  for the same weld shape. In addition,  $K_{fmax}$  depends upon the shape of the weld and the type of loading to which it is subjected ( $\alpha$ ), and upon the size or scale of the weldment ( $t$ ).

Using Eq. 6 and the observed variation in fatigue properties with hardness (Fig. 4), Eq. 3 can be rewritten:

$$S_a = \frac{S_u + 344 - \sigma_r}{1 + 0.0015 \alpha S_u t^{1/2}} [2N_I]^{-\frac{1}{6} \log 2 (1 + 344/S_u)} \quad (7)$$

where:

$S_a$  is the fatigue strength at  $2N_I$  ( $R = -1$ ), and

$\sigma_r$  is the residual stress at weld toe.

The fatigue strength of steel weldments predicted by Eq. 7 is a function of  $S_u$  and is plotted in Fig. 6 for three assumptions of weld toe residual stress ( $\sigma_r$ ) at a fatigue life of  $10^6$  cycles.

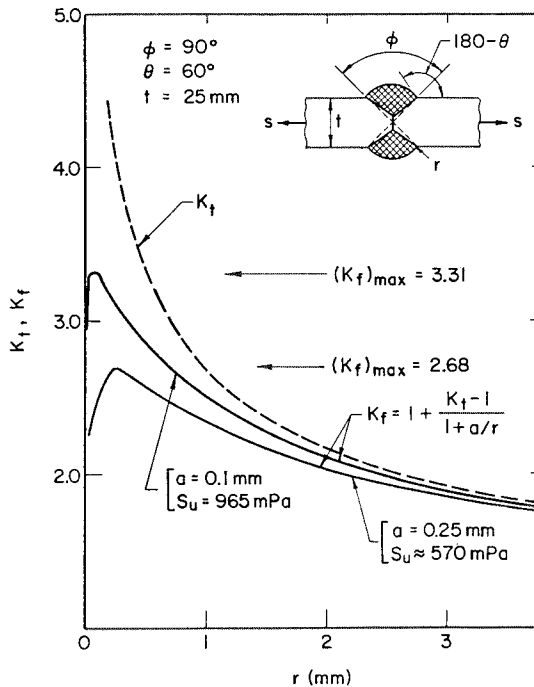


Fig. 5. Variations of  $K_{fmax}$  with strength level ( $S_u$ ) and consequent changes in the material parameter a.

For the assumption of no residual stress, it can be seen that the fatigue resistance of a steel weldment continues to increase with increasing  $S_u$  even though the increase in  $\sigma_f$  due to the increase in  $S_u$  is partially offset by a larger  $K_{fmax}$ . Under the assumption of positive residual stresses equal to the base metal yield strength ( $\sigma_r = +S_y$ ), the fatigue limit is no longer a strong function of  $S_u$  but increases only slightly and then, for the case considered, decreases with increases in  $S_u$  above 550 MPa. Thus, increasing the strength ( $S_u$ ) of weldments in the as-welded condition may actually decrease their fatigue strength due to the combined effects of increasing  $K_{fmax}$  and  $\sigma_r$ .

When the mean stress relaxes during cycling, the current value of mean stress ( $\sigma_0$ ) may be estimated by (6):

$$\frac{\sigma_0}{\sigma_{0S}} = (2N_i - 1)^k \tag{8}$$

where:

- $\sigma_0$  = current value of mean stress,
- $\sigma_{0S}$  = initial value of mean stress,
- $2N_i$  = elapsed reversals, and
- $k$  = relaxation exponent (a function of strain amplitude).

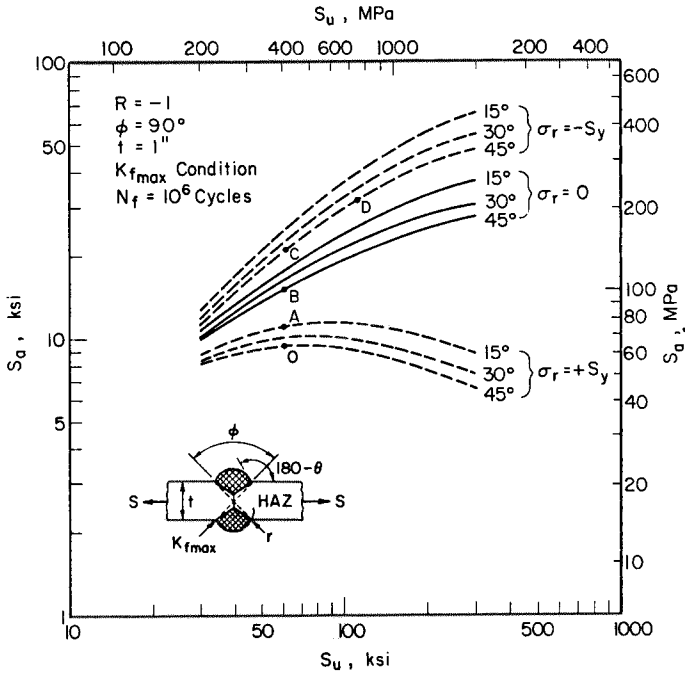


Fig. 6. Predicted influence of ultimate strength ( $S_u$ ) on the fatigue strength of a steel butt weld at  $10^6$  cycles.

Assuming that the notch-root strains are essentially elastic ( $2N_I > 2N_{tr}$ ) the damage per cycle is:

$$\frac{1}{2N_i} = \left( \frac{\sigma'_f}{\sigma_a} \right)^{\frac{1}{b}} \left( 1 - \frac{\sigma_0}{\sigma'_f} \right)^{\frac{1}{b}} \quad (9)$$

Using the Palmgren-Miner rule of cumulative damage and Eqs. 8 and 9, the fatigue crack initiation life under conditions of relaxing mean stress can be calculated by integrating the equation below and solving for the upper limit of integration using approximate methods (6):

$$\int_1^{2N_I} \left( \frac{\sigma'_f}{\sigma_a} \right)^{\frac{1}{b}} \left( 1 - \frac{\sigma_{0s}(2N_i)^k}{\sigma'_f} \right)^{\frac{1}{b}} d(2N_i) = 1 \quad (10)$$

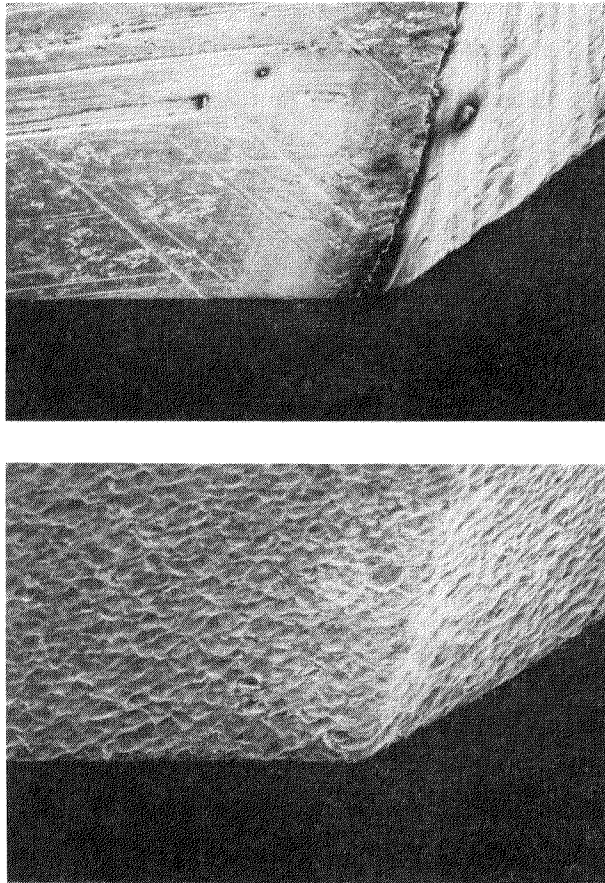


Fig. 7. Appearance of as-welded weld toe (above) and shot-peened weld toe (below) at 45x. (Scanning electron microscope micrographs)



The total fatigue life ( $N_T$ ) is considered to be the sum of the crack initiation life and the fatigue crack propagation life (Eq. 1). When initiation occurs at an obvious defect such as a pore, slag pocket or deep notch, the size of the initiated crack length ( $a_I$ ) may be taken as the dimension of the defect. Thus, the fatigue crack propagation life ( $N_p$ ) may be calculated taking the defect size as  $a_I$  and added to the estimate of  $N_I$  using Eq. 3 (naturally in the case of serious defects  $N_I$  may be rather short) to obtain  $N_T$ . Problems arise in the instance of weld discontinuities such as weld toes which are serious defects but not deep notches. In this case, the value of the initiated crack length ( $a_I$ ) is not clear. It has been past practice to assume arbitrarily that  $a_I$  was .01-in. regardless of the stress level or the material (2). Recent work by Chen (7) has provided an alternative strategy for the definition of  $a_I$ . For fatigue failure to occur, an  $a_I$  just greater than the length of a non-propagating crack ( $a_{th}$ ) must be provided by the process of fatigue crack initiation. Thus, at long lives,  $a_I$  should be just a little larger than  $a_{th}$ .

#### INFLUENCE OF SHOT PEENING ON THE FATIGUE LIFE OF WELDMENTS

The analytical model discussed in the previous section provides a means of exploring ways to improve the fatigue resistance of weldments. Since the fatigue crack initiation life ( $N_I$ ) dominates at long lives for low  $K_t$  notches such as weld toes, the long life fatigue resistance of weldments can be improved principally by increasing  $N_I$ , that is by: reducing the severity of the critical notch (i.e., reducing  $K_f$  to values less than  $K_{fmax}$  or reducing the absolute value of  $K_{fmax}$  through the production of less severe weldment shapes); by controlling residual stresses; and by improving material properties. Thus reducing the height of the weld crown ( $\theta = 45^\circ \rightarrow 15^\circ$ ) should increase the fatigue strength from 0  $\rightarrow$  A in Fig. 6. Stress relief ( $\sigma_r = +S_y \rightarrow 0$ ) should increase the fatigue strength from 0  $\rightarrow$  B. Over-stressing in tension should induce compressive residuals ( $\sigma_r = +S_y \rightarrow -S$ ) and increase the fatigue strength as much as from 0  $\rightarrow$  C, while shot peening should increase the strength of the material in the region of fatigue crack initiation and induce very large compressive residual stresses and thus result in the largest of the above improvements, 0  $\rightarrow$  D.

To apply the analytical model for weldment fatigue life it is assumed that the  $K_{fmax}$  condition occurs for shot-peened weldments. Scanning electron microscope examinations of the peened weld toes have shown that the peened surfaces are very rough and consist of overlapping shot impact craters: see Fig. 7. The values of the compressive residual stresses induced by shot peening have been measured (8) and found to be a function of the initial hardness of the peened metal (Fig. 8). The fatigue properties  $\sigma_f'$ , b and k were estimated from the hardness of the peened material at the weld toe at a depth of 200  $\mu\text{m}$ : see Figs. 4 and 9.

#### FATIGUE TESTS ON SHOT-PEENED ASTM-A514 WELDMENTS

ASTM-A514 structural steel weldments were fabricated for a study of the effects of shot peening on fatigue resistance. The material properties are given in Tables 1, 2, and 3. The A514 steel plates were ground to remove mill scale. Bead-on plate weldments were fabricated by depositing a weld bead on one side of a steel plate using a semi-automatic GMA welding apparatus (process parameters are given in Table 4). Shot peening was performed on these weldments prior to final machining. Test pieces were saw-cut from the welded and post-welded treated plates and machined to dimensions shown in Fig. 10. Shot peening of the weld toe region was performed by a local shot peening company. Total peening coverage was insured by Peenscan (8). All process parameters suggested by the shot peening company are listed in Table 5.

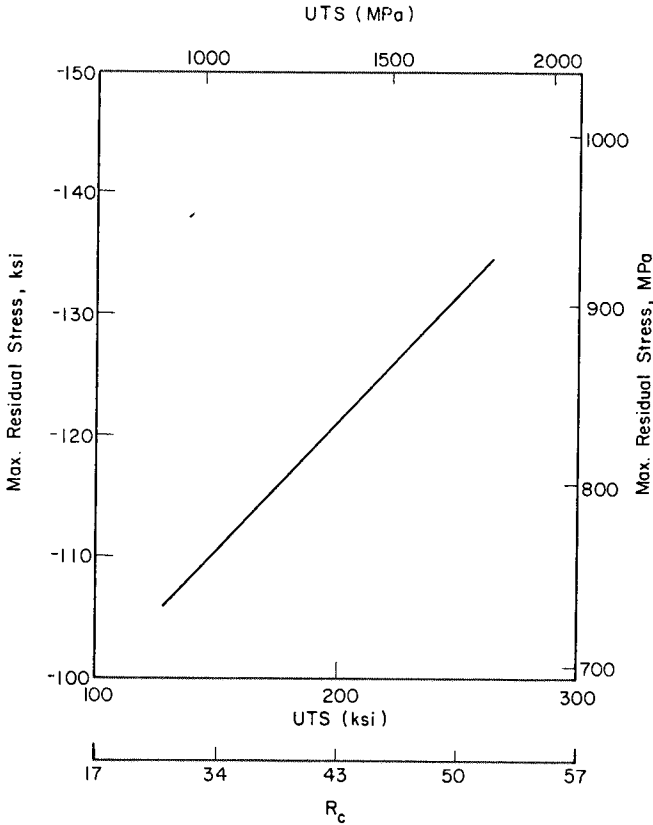


Fig. 8. Relationship between ultimate strength and maximum residual stress induced by shot peening (8).

TABLE 1 Chemical Compositions of Base Metal and Welding Electrode

Element (%)	Base Metal	Welding Electrode
	A514*	E110*
C	.16	.08
Mn	.82	1.70
P	.012	.005
S	.019	.009
Si	.23	.46
Cu	.27	---
Ni	.76	2.40
Cr	.54	.05
Mo	.47	.50
V	.06	.02
B	.004	---
Al	---	.003
Ti	---	.025

\*Ladle compositions supplied by the manufacturers

TABLE 2 Mechanical Properties of Base, Weld, and Heat-Affected Materials

Material	A514-BM	A514-HAZ	E110-WM
Hardness, DPH/BHN	320/303	496/461	382/362
Modulus of Elasticity, E (MPa)	209,000	209,000	209,000
0.2% Offset Yield Strength, (MPa)	889	1179	834
Ultimate Tensile Strength, $S_u$ (MPa)	938	1407	1034
Percent Reduction in Area, %RA	63.0	52.7	57.6
True Fracture Strength, $\sigma_f$ (MPa)*	1489/1269	2248/1986	2206/1910
True Fracture Ductility, $\epsilon_f$	0.994	0.750	0.857
Strain Hardening Exponent, n	0.994	0.092	0.092
Strength Coefficient, K (MPa)	1186	2210	1558

\* The first value is the load just before it is suddenly decreased prior to fracture divided by the final area of the fracture specimen. The second value is corrected for triaxial stress due to necking as proposed by Bridgmen.

TABLE 3 Cyclic and Fatigue Properties of Base, Weld, and Heat-Affected Materials

Material:	A514-BM	A514-HAZ	E110-WM(1P)
Cyclic Yield Strength, 0.2% (MPa)	604	938	649
Cyclic Strain Hardening Exponent, $n'$	0.091	0.103	0.177
Cyclic Strength Coefficient, $K'$ (MPa)	1089	1765	2020
Fatigue Strength Coefficient, $\sigma_f'$ (MPa)	1303	1999	1889
Fatigue Ductility Coefficient, $\epsilon_f'$	0.975	0.783	0.848
Fatigue Strength Exponent, b	-0.079	-0.087	-0.115
Fatigue Ductility Exponent, c	-0.699	-0.713	-0.734
Transition Fatigue Life, $2N_t$	346	1138	1536

TABLE 4 Welding Parameters

Parameter	Welding
Plate Thickness (mm)	12.7
Electrode Diameter (mm)	1.59
Voltage (V)	30
Current (amps)	290
Travel Speed (mpm)	0.43
Preheat Temp (°C)	96
Heat, Input (kJ/mm)	1.2
Shielding Gas	Ar-2% O <sub>2</sub>

TABLE 5 Shot-Peening Parameters

Air jet nozzle size (mm)	6.35
Shot nozzle size (mm)	12.7
Angle of impingement	45°
Air pressure (MPa)	0.55 ± 0.07
Length of cycle (mm)	100
Cycle time (min)	5
Shot size (mm)	0.84

\*Recommended and performed by commercial shot peening company

Two Micro-Measurements strain gauges (6.3 mm, 120  $\Omega$ ) were attached to both sides of each specimen to monitor bending stresses. A proper distance from the weld toe to the strain gauges was maintained to guarantee that the monitored strains would be independent of the weld toe stress concentration and would approximate the nominal surface strain.

Specimens were fatigue tested in a 100 kip MTS machine under load control ( $R=0$ ) at 5 Hz. The bending strain due to nominally axial loading was measured under small axial loads prior to cycling and any bending strain was reduced by forcing the grips and specimens into alignment through minor grip adjustments. In this manner, the bending stresses were reduced to less than 2% of the axial stresses. The fatigue test results of treated A514/E110 weldments are shown in Fig. 11.

Regions of interest were examined with SEM and optical microscope to characterize microstructures, toe geometries, and crack initiation sites. Micro-hardness traverse were performed on several of the peened weldments (Fig. 9). Peening produced no observable changes in the microstructure but induced a great increase in hardness at approximately 500  $\mu\text{m}$  below the surface. SEM investigations of weld toes showed sufficient surface discontinuities to use the  $K_f(\text{max})$  condition for all cases (Fig. 7). Fatigue failures initiated at the original weld toes.

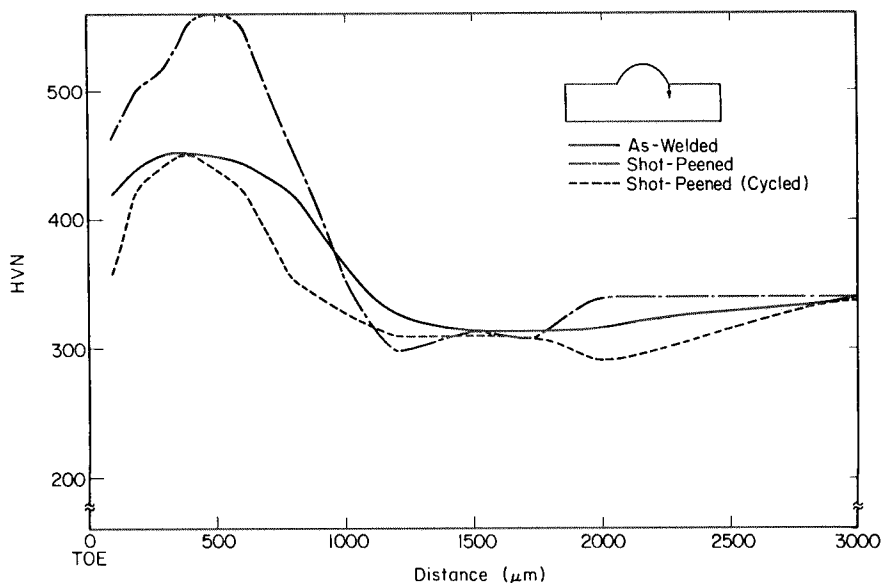


Fig. 9. Vickers hardness (VHN) inward from the weld toe for as-welded and (cycled and uncycled) shot-peened specimens.

A comparison of the experimental results and predictions of the effects of shot peening on the fatigue resistance of ASTM A514 weldments using Eqs. 1 and 10 is given in Fig. 11. The predicted lives of the shot-peened and as-welded specimens agree well with the experimental observations.

#### THE CONCEPT OF MAXIMUM RECOVERABLE LIFE

The maximum possible improvement in weldment fatigue life (maximum recoverable life or MRL) can be predicted using the analytical model discussed (Eq. 3):

$$2N_I^P = \left[ \frac{\Delta S K_f^P}{2(\sigma_f^{iP} - \sigma_0^P)} \right]^{\frac{1}{b_P}} \quad (11)$$

$$2N_I^W = \left[ \frac{\Delta S K_f^W}{2(\sigma_f^{iW} - \sigma_0^W)} \right]^{\frac{1}{b_W}}$$

when:

- $2N_I^P, 2N_I^W$  = Initiation life of plain plate and weldment, respectively,  
 $K_f^P, K_f^W$  = Fatigue notch factor for plain plate and weldment, respectively,  
 $\sigma_f^{iP}, \sigma_f^{iW}$  = Fatigue strength coefficient for plain plate and weldment HAZ, (after post weld treatment) respectively,  
 $\sigma_0^P, \sigma_0^W$  = Mean stress for plane plate and weld toe, respectively,  
 $b_P, b_W$  = Fatigue strength exponent for plane plate and weldment HAZ, respectively, and  
 $\Delta S$  = Remote stress range.

The maximum recoverable life (MRL) is:

$$\text{MRL} = 2N_I^P - 2N_I^W \approx 2N_T^P - 2N_T^W \quad (12)$$

Assuming  $b_P = b_W$ , the best possible weldment performance will occur when the maximum recoverable life is reduced to zero through manipulation of  $\sigma_0$  (i.e.,  $\sigma_r$ ),  $K_f$ , or  $\sigma_f^i$ . For this condition:

$$\frac{K_f^W}{K_f^P} < \frac{\sigma_f^{iW} - \sigma_0^W}{\sigma_f^{iP} - \sigma_0^P} \quad (13)$$

Now  $\sigma_0^P = K_f^P S_0$  and

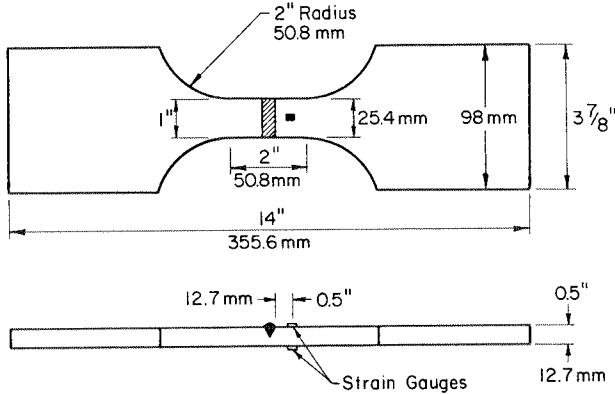


Fig. 10. Dimensions of specimens for fatigue testing of as-welded and shot-peened bead-on-plate weldments.

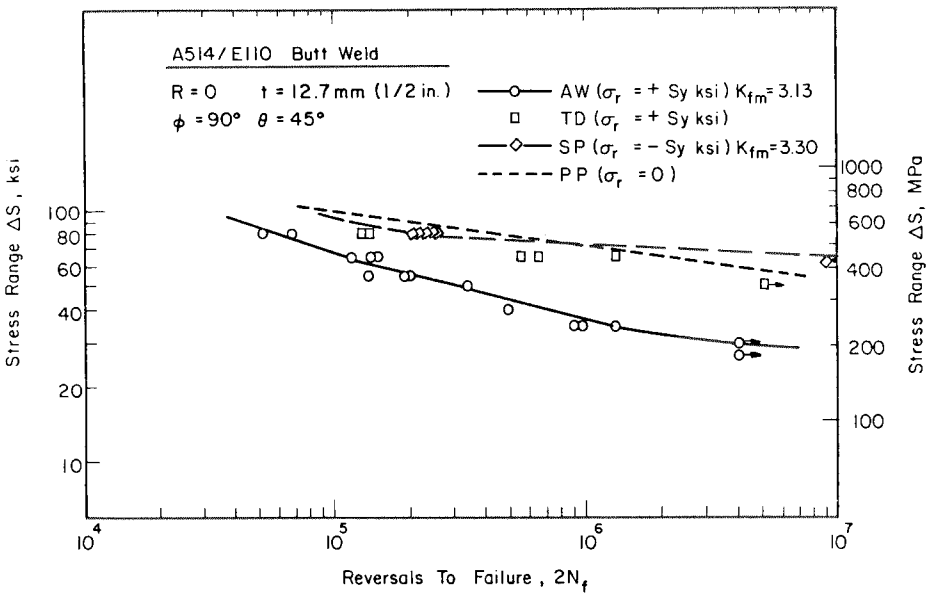


Fig. 11. Total fatigue life predictions for shot-peened and as-welded ASTM A514/E110 bead-on-plate weldments together with experimental results for T.I.G. dressed, shot-peened and as-welded bead-on-plate weldments.

$$\sigma_0^W = K_f^W S_0 + \sigma_r \tag{14}$$

where:

$S_0$  = remotely applied mean stress and

$\sigma_r$  = weld toe residual stress.

Therefore, Equations 13 and 14 result in:

$$\frac{K_f^W}{K_f^P} < \frac{\sigma_f^W - \sigma_r}{\sigma_f^P} \quad (15)$$

Equation 15 shows the quantitative relation between the three controllable factors for completely regaining the recoverable fatigue life (MRL = 0) and implies that recovery does not depend on stress range ( $\Delta S$ ) or R (=  $S_{min}/S_{max}$ ) ratio, but strongly depends on the factors of geometry ( $K_f$ ), residual stress ( $\sigma_r$ ) and material property ( $\sigma_f^P$ ).

If Eq. 15 is applied to several post-weld treatments for improving weld fatigue life, assuming that  $\sigma_f^W \approx 1.5 \sigma_f^P$ , the ranges of  $K_f^W/K_f^P$  which will permit the maximum possible improvement in weldment fatigue life are given in the table below:

TABLE 6 Estimated Effect of Post Weld Treatments

Treatment	$\sigma_r$	Range of $K_f^W/K_f^P$ for MRL = 0
stress relief	0	1 → 1.5
over stressing	$-\sigma_y \approx -\frac{S_{UBM}}{2}$	1 → 2
reduction in $K_f$	$\sigma_y \approx \frac{S_{UBM}}{2}$	1 <sup>+</sup>
shot-peening	$-0.5 \sigma_f^W$	1 → 3

The fatigue notch factor ( $K_f$ ) can be reduced to values less than  $K_{fmax}$  by laser or TIG dressing which treatments makes  $K_f^W$  at the new toe nearly equal to the  $K_f^P$  and thereby give complete recovery. Shot-peening is particularly effective in increasing the fatigue life of a weldment up to its plain plate life for ratios of  $K_f^W/K_f^P$  in the range 1 to approximately 3.

#### ACKNOWLEDGEMENTS

This study was principally supported by the University of Illinois Fracture Control Program which is funded by a consortium of midwest industries.

The authors wish to thank Professor JoDean Morrow of the Department of Theoretical and Applied Mechanics for his advice and help and Patrick Murzyn for his help in the experimental portions of the study and for providing the SEM micrographs.

The authors are particularly indebted to the Metal Improvement Company (Chicago Division) for shot peening the weldments and supplying a great deal of technical information on the shot-peening process.

## REFERENCES

1. Radziminski, J. B., Srinivansan, R., Moore, D., Thrasher, C. and W. H. Munse, (1973). Structural Research Series No. 405, University of Illinois at U-C., Urbana, IL.
2. Lawrence, F. V., Jr., Mattos, R. J., Higashida, Y. and J. D. Burke (1978). ASTM STP, 648, 134-158.
3. Higashida, Y., Burk, J. D. and F. V. Lawrence, Jr. (1978). Strain-Controlled Fatigue Behavior of a STM A36 and A514 Grade F Steels and 5083-0 Aluminum Weld Materials. Welding Journal, 57, 334s-344s.
4. Basquin, O. H. (1910). The Exponential Law of Endurance Tests. Proc. ASTM, 10, 625.
5. Lawrence, F. V. Ho, N-J, and P. K. Mazumdar (1981). Predicting the Fatigue Reistance of Welds. Ann. Rev. Material Sci., 11, 401-425.
6. Burk, J. D. and F. V. Lawrence, Jr. (1978). Fracture Control Program Report No. 29, University of Illinois at Champaign-Urbana, Urbana, IL.
7. Chen, W. C. and F. V. Lawrence, Jr. (1979). Fracture Control Program Report No. 32, University of Illinois at Urbana-Champaign, Urbana, IL.
8. Shot Peening Applications (1980), 6th ed., Metal Improvement Co., Inc. Paramus, NJ.